

## Characterisation of a new three-dimensional absolute optical position sensor and investigation on position and axis errors of a precision bearing on nm and $\mu\text{rad}$ scales.

Stefan Kubsky<sup>1</sup>, Antoine Loncle<sup>1</sup>, Thanh-Liem Nguyen<sup>2</sup>, Francois Nicolas<sup>1</sup> and Olivier Acher<sup>2</sup>

<sup>1</sup>Synchrotron SOLEIL, L'Orme des Merisiers, F- 91192 Gif-sur-Yvette, France

<sup>2</sup>HORIBA France, Avenue de la Vauve, F-91120 Palaiseau, France

[stefan.kubsky@synchrotron-soleil.fr](mailto:stefan.kubsky@synchrotron-soleil.fr)

### Abstract

Position control down to the nm-level is a key requirement for a growing number of scientific and industrial applications [1]. In this paper, a new optical measurement system "nanoGPS OxyO"<sup>®</sup> [2] is characterised, providing three absolute coordinates ( $x, y, \varphi_z$ ) in real time. The accuracy lies in the nm-range for  $x, y$  and in the range of  $10\mu\text{rad}$  for  $\varphi_z$ . The systems' modularity permits for integration, including harsh environments, vacuum and cryogenic applications. Characterization is carried out with a dedicated experimental setup employing laser interferometry. Our experiments suggest that existing sample holder standards or functional devices (e.g. precision optics in vacuum) can be equipped with the nGPS-system, without redesign of the metrological system.

Keywords : optical measurement system, absolute, nanometer precision, position encoder

Nm-precise position information for linear displacements is currently provided by three classes of sensors: Interferometers, optical rulers and capacitive sensors. The figure of merit for each type comprises accuracy, time-resolution and range. The so-called "nGPS" position sensor belongs to a lesser known class of sensor based on taking the image of a patterned plate with encoded image information [3]. The pattern plate combines some codes (somewhat similar to QR codes) that provide low resolution spatial information, with patterns that provide superlocalization capability. Superlocalization [4] describes the capability to determine the position and orientation of an object with an accuracy that exceeds the resolution of its image, which is made possible when the object has a number of known features. It belongs to the more general family of superresolution techniques [4]. Additional details on the nGPS sensor system are provided elsewhere [2]. It is highly desirable to perform experimental assessment of the capabilities of such a sensor using commonly accepted methods.

### 1. Experimental details

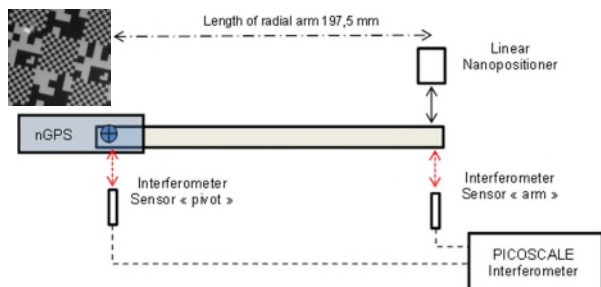


**Figure 1.** Schematic top view of experimental setup. The fiducial represents the rotation axis. The nGPS pattern is shown as insert.

The dedicated experimental setup is depicted schematically in Figure 1. The nGPS read-head includes a CMOS-camera (Basler aca 1920-40 $\mu\text{m}$ ) and a 10X lens (Edmund Optics, 10X, NA 0,28, WD 33,5mm). The patterned plate is a glass plate bearing lithography-defined patterns. A radial arm is fixed on a fluid dynamic bearing (FDB) originating from a hard disk drive.

The length of this horizontal arm is 197,5mm. At its end, a nanopositioning device (SMARACT SLC17xx series) with a nominal resolution of 100nm is attached via a small flexure element. Opposite to this element, a mirror faces the sensor ("arm") of a laser interferometer (SMARACT Picoscale). A second interferometer sensor ("pivot") is targeting another mirror close to the axis of rotation, in line with the x-axis of the nGPS, measurement distance in air is 39mm for both channels. The interferometer provides nm-resolution and sufficient time resolution to act as a reference for the nGPS. Both, the nGPS and the pivot arm are mounted on individual xyz manual positioning units.

The complete setup is mounted on an optical breadboard in an enclosure with passive vibration isolation and cable intercepts. Inside the enclosure, temperature, pressure and humidity are measured over time with mK resolution. Interferometer measurements are corrected for these environmental factors in real time down to ppm level.

Prior to measurements with the nGPS, drift induced by residual temperature gradients was determined. A maximum temperature gradient of -60mK/h has been observed during the night, when the laboratory is not heated. This temperature-drift results in +53; -7nm/h for channels "arm" and "pivot" respectively. These values represent the worst case scenario, when heating is off. Experiments have been carried out in more favourable conditions and during only a few minutes each (except for noise and stability). For these reasons, thermal drift is not taken into account.

### 2. Experimental results

#### 2.1. Characterisation of the nGPS sensor

Table 1 lists the rms-noise per channel. The comparison of nGPS and interferometer data suggests that the environmental noise level is slightly below 5nm. Image size used by the nGPS has been varied. Smaller images allow faster software treatment for position determination, and therefore allow faster sample rates. Lower noise levels are observed for larger images on nGPS and can go down to 1,4nm and 8  $\mu\text{rad}$ . A

qualitative interpretation is that larger image may allow better superlocalization performance. As the pattern images are far from perfection due to the presence of dust (Fig.1) these figures could be possibly improved, but are sufficient for the present purpose.

**Table 1.** Noise figures of the different sensors

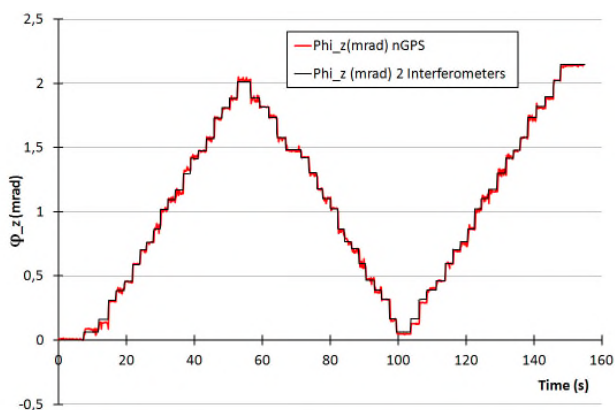
nGPS	read rate (Hz)	noise (rms)		
		X(nm)	Y(nm)	$\varphi_z$ ( $\mu$ rad)
Large Image (2,3M Pixels)	4	1,4	4,0	8,0
Medium Image (0,6 MPix)	15	2,6	3,3	17,4
Small Image (0,26 MPix)	30	4,6	4,6	20,8

Interferometer	read rate	noise (rms) d (nm)
Pivot	>10kHz	0,5
Arm End	>10kHz	4,6

## 2.2. Small angle rotation analysis on a Fluid Dynamic Bearing (FDB)

The experimental setup design permits for a characterisation of dynamic and static movements. A series of 20 linear movements in steps of 25 $\mu$ m at the "arm" sensor has been effectuated by the smaract nanopositioner. The resulting change in angle at the pivot point has been simultaneously recorded by the nGPS. The effective angle change resulting from the linear movement at "arm" has been calculated from the interferometer data. Figure 2 shows a good match between the angle as measured by the nGPS and the interferometer. Observable deviations are comprised in an interval of less than 100 $\mu$ rad. A more detailed measurement (not shown here) reveals angular errors to be below 15 $\mu$ rad. This is consistent with results from 2.1.



**Figure 2.** Angle measured in 20 steps simultaneously by nGPS and interferometer.

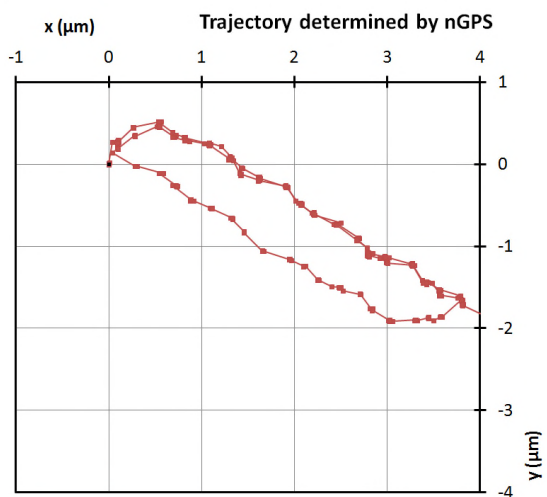


**Figure 3.** Rotation axis position during 20 steps measured by nGPS during 3 cycles, see Fig2.

For a perfect rotation, the trajectory observed by nGPS should show a circle for a full rotation and a circle segment for a partial rotation. In Figure 3 however, a hysteresis is observable. The opening of the hysteresis loop of about 500nm corresponds to the radial displacement of the bearings' axis. Since the bearing is an FDB, this observation is in good agreement with the construction properties: This type of bearings are not made for quasistatic and angularly small movements, the fluid film between rotor and stator moves and brings them up to contact, as observed by the measurement. As more than one cycle has been measured, the fair repeatability of the hysteresis loop is a good indicator for the quality of the measurement and the fluid-gap of the bearing.

## 3. Discussion

Both types of sensors give complementary information on the examined scales. Technologically, the novel feature of the nGPS, namely to produce three absolute coordinates ( $x, y, \varphi_z$ ) in real time has been confirmed and quantified. The comparison with interferometric data shows a clear dependence of noise with increasing sampling rate.

Very small angular displacements down to 15 $\mu$ rad can readily be measured by nGPS as an alternative to well-known optical rulers. Small, nanosystem-compatible commercial rotary stages have a typical resolution in the 10-20 $\mu$ rad range. The new sensor system can thus be employed for such systems, but in a different geometry, and closer to the point of interest (measure on sample). Specifically flexure-based precision mechanics can profit from the unique nGPS ability to trace precisely both translation ( $xy$ ) and rotation  $\varphi_z$ .

The experimental setup still introduces mechanical instabilities which interfere with the interpretation of some of the results, a more rigid version is actually under construction.

The axis displacement determination on a precision FDB bearing is an example for the applicability of the nGPS.

## 4. Conclusion

A new type of absolute position sensor with nm resolution and simultaneous real-time readout of three coordinates has been characterised. Noise and repeatability have been compared to interferometers and are consistent. As one example, an investigation on precision bearings has been performed and analysed.

The nGPS permits for integration into complex systems, alleviating the necessity to integrate active components (optical rulers), or bulky sensors (capacitive) or highly linear movements (interferometers) for the desired axes. Compact size and modularity pave the way for both industrial and scientific applications.

## References

- [1] Fleming A.-J. "A review of nanometer resolution position sensors: Operation and performance"; *Sensors and Actuators A* **190** (2013) 106–126.
- [2] Acher O. et Podzorov A. patent: US 9736389 and "An absolute sample position referencing solution for convenient cross-platform observations; application to the assessment of microscope stability and translation stage reproducibility"; DOI: 10.1002/9783527808465.EMC2016.6127
- [3] Sandoz P., Bonnans V. and Gharbi T. "High-accuracy position and orientation measurement of extended two-dimensional surfaces by a phase-sensitive vision method"; *Applied Optics* **41**, 5503-5511 (2002)
- [4] Cremer, C. & Masters, B. "Resolution enhancement techniques in microscopy", *EPJ H* (2013) 38: 281. <https://doi.org/10.1140/epjh/e2012-20060-1>